ACS Sustainable Chemistry & Engineering

pubs.acs.org/journal/ascecg

Research Article

Heat, Electricity, and Fuel Gas Ploy-Generation System on an Island based on Plastic Waste Gasification in Supercritical Water

Weizuo Wang, Cui Wang, Yong Huang, Huaiyu Lu, Jia Chen, Jinwen Shi,* and Hui Jin*

Cite This: https://doi.org/10.1021/acssuschemeng.2c04115

Read Online

ACCESS | Metrics & More | Article Recommendations | Supporting Information

ABSTRACT: Plastic pollution in the ocean has become a serious threat to the health of marine life and even terrestrial life. It is also a challenge to transport it landside for recycling. A system to recycle the plastics in situ on an island was proposed with the aim to convert the plastics to fuel gases, such as H_2, CH_4, and CO. As one of the most abundant thermoset plastics in the ocean, epoxy plastics were recycled in this system. They were gasified in supercritical water driven by concentrated solar energy. A heat exchanger and turbine were used for electricity. The fuel gas could be stored in the gas tank at 4 MPa. The energy and exergy efficiency in this system were analyzed, and the effects of temperature, pressure, and feedstock concentration were discussed. The typical conditions were as follows: temperature 600 °C; pressure 25 MPa, and feedstock concentration 5 wt %. The mole fractions of these products were 48.13%, 22.97%, 0.84%, and 28.06%, respectively. Additionally, the energy and exergy efficiency were 51.75% and 45.22%, respectively.

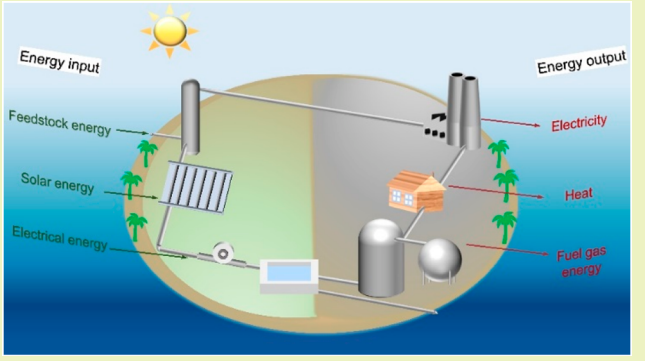

KEYWORDS: *supercritical water gasification, epoxy plastics, ploy-generation system, flue gas production, energy and exergy efficiency, optimal operating condition*

1. INTRODUCTION

Plastics have caused a lot of pollution, which seriously threaten the marine environment and ecosystem. It has been econfirmed that plastics can be found in the oceans all over the world.[1−4] One study assessed the quality and quantity of macrodebris and microplastics at six beaches in 2014.[5] It was found that plastics accounted for over 64% of the macrodebris and microplastics were ubiquitous. Plastics could also be found at the most remote beaches in the North Pacific.[6] Even worse, plastics, especially microplastics, are accumulating in terrestrial and aquatic systems, becoming an emerging problem in scientific and social areas.[7]

Traditional methods to deal with plastics used to be divided into three types,[8,9] sanitary landfill, burning, and recycling. Sanitary landfill and burning also caused a lot of pollution. Therefore, recycling was regarded as the best way to deal with plastics in the future.

Different from thermoplastics, glass, and metals, thermoset plastics were thought to be difficult to recycle or reuse because of their excellent physical and mechanical properties.[10] However, this view changed as methods such as hydrolysis and glycolysis were proven to successfully recycle thermoset plastics.[11] It has also been difficult to dry microplastics from the ocean. As a result, technology that can recycle or reuse plastics without dewatering or drying has been considered. Microplastics floating on the ocean could be gasified by supercritical water on an island. In this way, elements that easily form acids could be converted into harmless inorganic salts and the emission of pollutants such as NO_x and SO_x could be avoided. The special flow and heat transfer characteristics of supercritical water played a positive role in the promotion of gasification reaction. In addition, the process of dewatering and drying for feedstocks was avoided in this way.[12] Great cost savings could be achieved using this technology.

As an island energy system, many challenges, such as the weak connection to the mainland, congestion, and stability problems need to be resolved, and hydrogen technologies could be the key to these problems.[13] Hydrogen-rich syngas, as the main products of supercritical water gasification could fit the island energy system well and become the main type of energy generation in this system. In addition to these challenges of output, the limit of input energy was also considered. Solar energy was a viable energy alternative.[14,15] In the system of supercritical water gasification, external heat supply in the processes of heating water to supercritical and

Received: July 10, 2022
Revised: August 19, 2022

maintaining constant temperature in the reactor could be obtained by concentrated solar energy.

Therefore, a solar-powered poly generation system could be envisaged, in which plastics collected nearby in the ocean were used to cogenerate electricity, heat, and gas. It was expected to have many application scenarios on the island. The thermochemical analysis of such a system was seldom analyzed.

This work focused on a system on the island based on plastics gasification in supercritical water, in which fuel gases such as H_2, CH_4, and CO were produced. Epoxy plastics and water were heated by solar energy and a pump provided the pressure of the reaction, while electricity, heat, and fuel gas were generated continuously in the pipelining system. The working conditions of gasification, such as temperature, pressure, and the feedstock concentration, were changed, and then their effects on products distribution, energy efficiency, and exergy efficiency could be investigated, respectively.

2. EXPERIMENTAL SECTION

2.1. Materials. Epoxy plastics, the most abundant thermoset plastic in the ocean,[16] were widely used in adhesives, coatings, shells, and other fields.[17] The chemical structure was shown in Figure 1. It

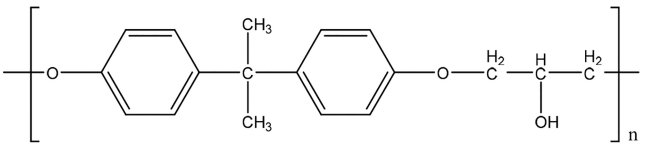

Figure 1. Chemical structure of epoxy plastics.

was shown that there were eight degrees of unsaturation (double benzene ring) in the monomer. As a result, large quantities of permanent gas, such as CO and CH_4, would be released during pyrolysis.[18]

The elemental and proximate analysis of epoxy plastics (EP) measured in the laboratory was shown in Table 1. The migration of N and S elements was a significant method for studying the mechanism of gasification, and many researchers have investigated the migration of N and S elements.[19−23] However, the deviation between the two results was not obvious in this paper. In addition, the mass fraction of N or S was lower than 1 wt %. Therefore, the existence of N and S elements was ignored in this paper. Three elements of C, H, and O in the pure epoxy plastic account for 76.06, 7.04, and 16.29 wt %, respectively, according to the structural formula.

2.2. Structure of System. It was proven that plastics could be gasified in supercritical water and the gas products were made up of CO_2 and flammable gas, such as H_2, CH_4, and CO.[24−29] As a result, products in gas phase after the gasification consisted of H_2, CH_4, CO, CO_2, and H_2O. And the physical energy and chemical energy of these products could be recycled and stored in the form of electricity, heat, and fuel gas. The flowchart of the system was shown in Figure 2. Contents in each flow were shown in Table 2. The process of the system and measurement parameters were discussed in detail in the Supporting Information (SI.2).

3. RESULTS AND DISCUSSION

In this investigation, the typical conditions were as follows: temperature of 600 °C; pressure of 25 MPa; and feedstock concentration of 5 wt %. On this basis, the temperature changed in the range of 540 °C to 675 °C, the pressure would change from 23 to 29 MPa. The main mass flow, the sum mass flow of flow 1 and flow 4, was kept at 1000 kg/h. The feedstock concentration was 1 wt % to 9 wt %.

3.1. Effect of Reaction Temperature. The increase of reaction temperature led to the increase of the product yield from 81.59 kg/h at 540 °C to 105.43 kg/h at 675 °C, as shown in Figure S1. The conversion rate of hydrogen increased at the same time. It was explained that gasification was endothermic. As a result, the heat added into the reactor would promote the reaction and more water would be reacted. The mole fraction of H_2 increased from 33.33% at 540 °C to 55.85% at 675 °C, while the fraction of CH_4 decreased from 31.15% at 540 °C to 11.84% at 675 °C. The mole fraction of CO increased and that of CO_2 decreased. HE was 257.9% at 540 °C, and it increased to 323.9% at 675 °C. Research on lignocellulosic biomass components showed that temperature was the most dominant factor affecting the yield of products, especially the yield of H_2.[30]

On the one hand, free-radical reactions, such as the pyrolysis reaction, led to the release of $H^•$ from H_2O and the reaction. At the same time, ion reaction led to the conversion from $H^•$ to H_2O. The high temperature promoted the former while hindering the latter.[31,32] The released $H^•$ which did not convert to water would form the H_2 and CH_4. And HE would be associated with the $H^•$. On the other hand, the steam reforming reaction (s19) was endothermic,[33] promoted by the increase of temperature. The promotion caused the increase of the yield of the products. Methanation reactions (s21) and (s22) were exothermic and could be inhibited at high temperature.[34] As a result, the fraction of H_2 increased and that of CH_4 decreased as the temperature increased.

In this system, the type of turbine and the working condition of flow 8 changed with the increase of reaction temperature as shown in Table S1. The photothermal conversion efficiency, efficiency of the preheater and reactor, decreased with the increase of temperature according to (s15), and the temperature of flow 10 also changed. As a result, the generation and the efficiency of both the energy and exergy changed accordingly, as shown in Figure S2. The energy efficiency of the system increased with temperature, while the exergy efficiency decreased. The increase of energy efficiency and decrease of exergy efficiency were attributed to the change of turbine type.

Both energy input into and output from the system increased with reaction temperature, as shown in Figure S3A. The energy to preheat the plastics and water increased and the photothermal conversion efficiency, calculated by (s15), decreased with reaction temperature. Influenced by these factors, the solar energy absorption increased sharply. Meanwhile, heat recycled from the cooler (heat output) and the

Table 1. Elemental and Proximate Analysis of Epoxy Plastics

feedstock	elemental analysis (wt %)					proximate analysis (wt %)				
	C_{ad}	H_{ad}	N_{ad}	S_{ad}	O_{ad}[a]	M_{ad}	A_{ad}	V_{ad}	FC_{ad}	$Q_{net,ad}$ (MJ·kg^{-1})
epoxy plastics	75.06	7.188	0.07	0.984	16.288	0.36	0.05	90.45	2.15	31.19

[a]By difference; ad, air drying base; Q_{net}, net calorific value.

https://doi.org/10.1021/acssuschemeng.2c04115
ACS Sustainable Chem. Eng. XXXX, XXX, XXX−XXX

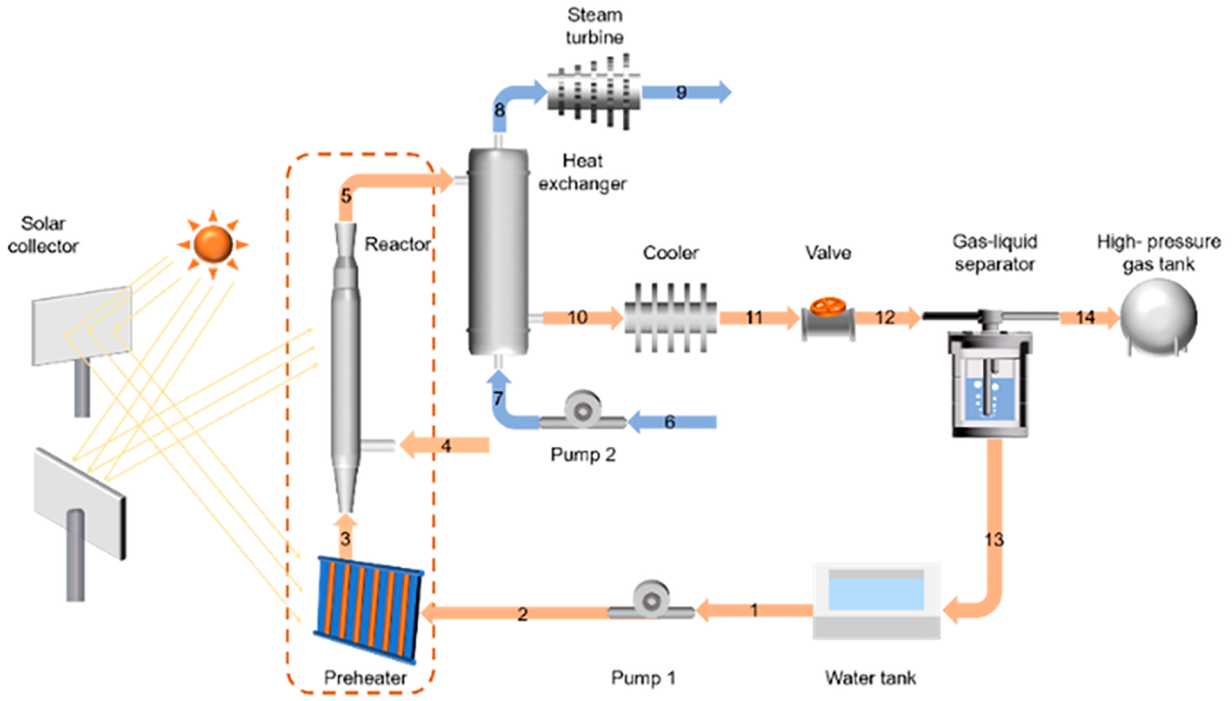

Figure 2. Flowchart of heat, electricity and fuel gas ploy-generation system. (Heat was recycled by cooler; electricity was produced by steam turbine; and fuel gas was collected in a high-pressure gas tank.)

Table 2. Contents in Each Flow of the System

number of flow	contents in the flow
1, 2, 3, 6, 7, 8, and 9	H_2O
4	plastics and H_2O
5, 10, 11, and 12	H_2, CH_4, CO, CO_2, and H_2O
13	H_2O with small amount of H_2, CH_4, CO, and CO_2
14	H_2, CH_4, CO, CO_2

energy stored in the products increased. The cooler could recycle more heat due to the increase of temperature in flow 10. The increase of reaction temperature promoted the gasification, which increased the yield of the products. As a result, the chemical energy stored in products increased. As a result, both the energy input into the system and the output from the system increased, and the energy efficiency increased with temperature.

The exergy efficiency of the system decreased with the increase of temperature in the ranges of 540 °C to 555 °C and 570 °C to 675 °C. The type of turbine changed from 555 °C to 570 °C, which caused the increase of exergy efficiency. Shown in Figure S3B, both the exergy generated from the system and the one cost in the system increased. The increase of temperature promoted the gasification and the chemical exergy contained in products increased. However, the high temperature made for significant heat input and low photo-thermal conversion efficiency, which could lead to substantial irreversible loss. As a result, the exergy efficiency generally decreased with temperature.

3.2. Effect of Reaction Pressure. It was shown in Figure S4 that the yield of products decreased as the pressure increased. The contents of CH_4 increased from 21.78% at 23 MPa to 25.21% at 29 MPa. The contents of other gases such as H_2 and CO_2 decreased from 49.37% to 45.80% and from 27.98% to 28.18%, respectively. HE was negatively correlated with the pressure. However, all the effects of reaction pressure could be neglected, which could be verified in experiments on supercritical water gasification.[31,35−37]

The reactions, with chemical equilibrium shown in (s19), (s20), (s21), and (s22), affected the contents of products. The steam reforming reaction (s19) would be inhibited with the increase of pressure, and it directly determined the mass flow of products. As a result, the yield of products decreased from 92.95 kg/h at 23 MPa to 89.29 kg/h at 29 MPa. The yield and contents of CH_4 were influenced by methanation reactions (s21) and (s22).[38] The increase of pressure would promote these reactions and increase the yield and contents of CH_4. Both the inhibition of the steam reforming reaction (s19) and the promotion of methanation reactions (s20) and (s21) would decrease the yield of H_2. Less water involved in the reaction increased the water vapor content in the reactor at the same time. The pressure could not influence the chemical equilibrium of reaction (s20) on its own. However, the increase of water vapor and the decrease of H_2 promoted the reaction (s20). As a result, the yield of products decreased and the mass of water vapor increased. The mole fraction of H_2 and CO decreased while that of CH_4 and CO_2 increased.

It was shown in Figure S5 that the efficiency of both energy and exergy changed slightly with pressure. It was shown in Figure S6A that the work of pump increased with pressure and the heat generated by the pump work also heated the flow.

https://doi.org/10.1021/acssuschemeng.2c04115
ACS Sustainable Chem. Eng. XXXX, XXX, XXX−XXX

Therefore, the work of pump increased and the solar absorption in the preheater decreased slightly because the pump work accounts for a small proportion of the input energy. As for the output of the system, the chemical energy in products decreased within 0.6% due to the slight change of the yield of products shown in Figure S4. Electricity produced from the turbine did not change with pressure, and the recycled heat at different pressures was a similar value. Therefore, the energy efficiency of the system changed slightly with pressure, and so did the exergy efficiency, as shown in Figure S6B.

3.3. Effect of Feedstock Concentration. The yield of each product increased with the increase of feedstock concentration, as shown in Figure S7. The product yields increased from 12.52 kg/h at 1 wt % to 162.33 kg/h at 9 wt %. However, the amount of the gas produced per kilogram of sample decreased at the same time. The mass flows of H_2 and CO_2 per kilogram of sample were greatly reduced while CH_4 increased slightly. HE decreased significantly from 408.12% to 254.62% when the feedstock concentration increased from 1 wt % to 9 wt %.

The mole fractions of products also greatly changed with the feedstock concentration. The content of H_2 decreased significantly with the increase of feedstock concentration, while that of CH_4 increased sharply. The contents of CO and CO_2 also increased. The increase of feedstock concentration indicated a decrease in the density of water.[36,39] According to the numerical study of Zhao et al., the diffusion coefficient was proven to have a negative power relation with the density of water.[40] The decrease in the density of water meant weaker and fewer hydrogen bonds and molecules could move more freely.[41] The static dielectric constant and the viscosity would subsequently decrease.[42] Therefore, the reaction was inhibited at high feed concentration.

It was shown in Figure S8 that both the energy efficiency and exergy efficiency increased with the feedstock concentration, and the growth trend slowed down gradually. Energy in plastics increased with feedstock concentration. With the increase of mass flow in flow 4 and the decrease of that in flow 1, both the work of pump and solar energy absorbed from the system decreased, while the solar energy absorbed in the reactor increased as shown in Figure S9. Meanwhile, the yield of fuel gas increased sharply which increased the chemical energy in products. However, the decrease of conversion rate slowed down the trend. In general, both the energy input and the energy output increased with feedstock concentration. The energy efficiency also increased. The change of exergy efficiency had a similar trend.

4. INVESTIGATION ON OPTIMAL OPERATING CONDITION

The yield of products and the efficiency of the system were influenced by temperature and feedstock concentration. However, the influence of temperature on the efficiency was not monotonous. The efficiency increased with feedstock concentration but the growth trend slowed down. The cost of energy also increased at the same time. Therefore, it was necessary to find the optimal operating condition of the system. 80 different working conditions at 4 temperatures (570 °C, 600 °C, 630 °C, 660 °C), 4 pressures (23 MPa, 25 MPa, 27 MPa, 29 MPa), and 5 feedstock concentrations (1 wt %, 3 wt %, 5 wt %, 7 wt %, 9 wt %) were investigated and compared. The yield of fuel gas and efficiency of the system were calculated to find the optimal operating condition.

4.1. Optimal Operating Condition for Production of Gas. As the physical products of the system, the yield of fuel gas could reflect the rate of plastics reuse. The yield and conversion rate of hydrogen were investigated in this section.

The yield of gas was shown in Figure S10. The yield of H_2 increased slowly when the feedstock concentration reached 5 wt %. Hydrogen atoms would mainly tend to generate CH_4 at high concentration. Meanwhile, HE increased with temperature and decreased with feedstock concentration as shown in Figure S11. The promotion of temperature on HE was the most obvious at 5 wt % due to the methanation trend at high concentration. The influence of pressure on the yield of H_2 and HE could be neglected. As a result, both the yield of H_2 and HE could reach a high level at 660 °C, 23 MPa, and 5 wt %.

4.2. Optimal Operating Condition for Efficiency. The efficiency of energy and exergy would reflect the performance of system. The optimal operating condition for efficiency was investigated in this section.

It was shown in Figure S12 that the energy efficiency increased with temperature. As a result, the maximum energy efficiency in these conditions was 60.42% at 660 °C, 23 MPa, and 9 wt %.

Energy flow at the optimal operating condition for efficiency was expressed by the Sankey diagram shown in Figure S13. Energy loss percentages of each model were also displayed. It was found that turbine cost was the main loss of the system. The energy consumed by the steam turbine accounted for 70% of the energy loss. Nonisentropic processes and heat dissipation were the main factors leading to energy loss in the steam turbines, especially the latter. Electricity was the energy in high grade and the conversion efficiency from heat to electricity was low. The efficiency of the steam turbine was $\eta_{electric}$, which equaled 28.51%. As the main model to absorb solar energy, the preheater also lost a lot of energy, which contained about 16% of the total loss. The efficiency from solar to heat reached 86.69%. Heat lost in the heat exchanger accounted for about 11% of the whole loss. The energy efficiency of the heat exchanger was set to 90%. The inlet steam temperature of the industrial steam turbine was always lower than 535 °C due to some safety problems at starting, downtime, and loading. The temperature difference of the heat transfer increased with the reaction temperature when the inlet steam temperature reached its maximum. The increase of temperature difference caused more heat loss.

The exergy efficiency was shown in Figure S14. The exergy efficiency decreased with temperature and increased with feedstock concentration. Therefore, the maximum exergy efficiency was at the lowest temperature and the highest concentration in these conditions. The exergy efficiency reached 58.72%, the maximum value, at 570 °C, 29 MPa, and 9 wt %.

The exergy flow at this condition was also expressed by the Sankey diagram shown in Figure S15. The loss of solar energy accounted for 75% of the whole exergy loss in the system. The exergy efficiency of the preheater was 47.75% and that of the reactor was 64.64%. Exergy loss on the steam turbine accounted for 15% of the total exergy loss. The exergy efficiency of this model was 66.72% due to the internal efficiency. Just like the energy loss, the exergy loss in the heat exchanger accounted for 9% due to the temperature difference. And the exergy efficiency of the heat exchanger was 91.85%.

https://doi.org/10.1021/acssuschemeng.2c04115
ACS Sustainable Chem. Eng. XXXX, XXX, XXX−XXX

5. CONCLUSIONS

A system to clean up the plastics in the ocean was based on an island in this work, in which waste plastics could be converted into hydrogen-rich syngas. Heat and electricity could also be generated from the system. The gasification and hydrogen technology used in this system could solve many problems of the island energy system. The reactor corrosion by easily-forming-acids elements was avoided and the cost of dewatering and drying was saved. In this work, the effects of working conditions, such as temperature, pressure, and feedstock concentration, on both the mole fraction of the fuel gas and the system efficiency were simulated. The results were as follows:

1. High temperature, low pressure, and low concentration of plastics could increase both the yield and mole fraction of H_2 and decrease those of CH_4. Yield of products would increase with temperature from 81.59 kg/h at 540 °C to 105.43 kg/h at 675 °C. The yield also increased with feedstock concentration, from 12.52 kg/h at 1 wt % to 162.33 kg/h at 9 wt %. Meanwhile, the influence of pressure was neglected.

2. The energy efficiency of the system increased with temperature while the exergy efficiency decreased with temperature, except for the changing of turbine in the system. The energy efficiency increased from 51.18% at 570 °C to 52.44% at 660 °C, while the exergy efficiency decreased from 46.19% to 43.36%. The effect of pressure on the efficiency could be neglected. Both the energy efficiency and the exergy efficiency increased with the feedstock concentration and the growth trend slowed down.

3. The optimal operating conditions for production of gas were at 660 °C, 23 MPa, and 5 wt % with a high yield of H_2 and HE. The maximum energy efficiency reached 60.42% at 660 °C, 23 MPa, and 9 wt %, while the exergy efficiency reached 58.72% as the maximum value at 570 °C, 29 MPa, and 9 wt %.

ASSOCIATED CONTENT

Supporting Information

The Supporting Information is available free of charge at https://pubs.acs.org/doi/10.1021/acssuschemeng.2c04115.

SI.1, Abbreviation table; SI.2, process of the system and measurement parameters; SI.3: (Figures S1, S4, and S7) influence of temperature, pressure, and feedstock concentration on gas yield and mole fraction; (Figures S2, S5, and S8) influence of temperature, pressure, and feedstock concentration on the energy and exergy efficiency of the system; Figures S3, S6, and S9) energy and exergy distribution at different temperature, pressure, and feedstock concentration; (Figure S10) gas yield at different conditions; (Figure S11) conversion rates at different conditions; (Figures S12 and S14) energy and exergy efficiency at different conditions; and (Figures S13 and S15) energy flow of the system at the optimal operating condition; and SI.4: (Table S1) match of general turbine parameters and reactor temperature (PDF)

AUTHOR INFORMATION

Corresponding Authors

Jinwen Shi − *State Key Laboratory of Multiphase Flow in Power Engineering (SKLMF), Xi'an Jiaotong University, Xi'an, Shaanxi 710049, P. R. China;* orcid.org/0000-0001-7291-2840; Phone: +86 029 82668767; Email: jinwen_shi@mail.xjtu.edu.cn

Hui Jin − *State Key Laboratory of Multiphase Flow in Power Engineering (SKLMF), Xi'an Jiaotong University, Xi'an, Shaanxi 710049, P. R. China;* orcid.org/0000-0001-9216-7921; Phone: +86 029 82660876; Email: jinhui@mail.xjtu.edu.cn

Authors

Weizuo Wang − *State Key Laboratory of Multiphase Flow in Power Engineering (SKLMF), Xi'an Jiaotong University, Xi'an, Shaanxi 710049, P. R. China*

Cui Wang − *State Key Laboratory of Multiphase Flow in Power Engineering (SKLMF), Xi'an Jiaotong University, Xi'an, Shaanxi 710049, P. R. China*

Yong Huang − *State Key Laboratory of Multiphase Flow in Power Engineering (SKLMF), Xi'an Jiaotong University, Xi'an, Shaanxi 710049, P. R. China*

Huaiyu Lu − *State Key Laboratory of Multiphase Flow in Power Engineering (SKLMF), Xi'an Jiaotong University, Xi'an, Shaanxi 710049, P. R. China*

Jia Chen − *State Key Laboratory of Multiphase Flow in Power Engineering (SKLMF), Xi'an Jiaotong University, Xi'an, Shaanxi 710049, P. R. China*

Complete contact information is available at: https://pubs.acs.org/10.1021/acssuschemeng.2c04115

Notes

The authors declare no competing financial interest.

ACKNOWLEDGMENTS

This work was supported by the Basic Science Center Program for Ordered Energy Conversion of the National Natural Science Foundation of China (No. 51888103).

REFERENCES

(1) Kanhai, L. D. K.; Gardfeldt, K.; Krumpen, T.; Thompson, R. C.; O'Connor, I. Microplastics in sea ice and seawater beneath ice floes from the Arctic Ocean. *Sci. Rep.* **2020**, *10* (1), 5004.

(2) Barnes, D. K. A.; Morley, S. A.; Bell, J.; Brewin, P.; Brigden, K.; Collins, M.; Glass, T.; Goodall-Copestake, W. P.; Henry, L.; Laptikhovsky, V.; Piechaud, N.; Richardson, A.; Rose, P.; Sands, C. J.; Schofield, A.; Shreeve, R.; Small, A.; Stamford, T.; Taylor, B. Marine plastics threaten giant Atlantic Marine Protected Areas. *Curr. Biol.* **2018**, *28* (19), R1137−R1138.

(3) Patti, T. B.; Fobert, E. K.; Reeves, S. E.; Burke da Silva, K. Spatial distribution of microplastics around an inhabited coral island in the Maldives, Indian Ocean. *Sci. Total Environ.* **2020**, *748*, 141263.

(4) Eriksen, M.; Maximenko, N.; Thiel, M.; Cummins, A.; Lattin, G.; Wilson, S.; Hafner, J.; Zellers, A.; Rifman, S. Plastic pollution in the South Pacific subtropical gyre. *Mar. Pollut. Bull.* **2013**, *68* (1), 71−76.

(5) Laglbauer, B. J. L.; Franco-Santos, R. M.; Andreu-Cazenave, M.; Brunelli, L.; Papadatou, M.; Palatinus, A.; Grego, M.; Deprez, T. Macrodebris and microplastics from beaches in Slovenia. *Mar. Pollut. Bull.* **2014**, *89* (1), 356−366.

(6) McDermid, K. J.; McMullen, T. L. Quantitative analysis of small-plastic debris on beaches in the Hawaiian archipelago. *Mar. Pollut. Bull.* **2004**, *48* (7), 790−794.

(7) Tirkey, A.; Upadhyay, L. S. B. Microplastics: An overview on separation, identification and characterization of microplastics. *Mar. Pollut. Bull.* **2021**, *170*, 112604.
(8) Bishop, G.; Styles, D.; Lens, P. N. L. Recycling of European plastic is a pathway for plastic debris in the ocean. *Environ. Int.* **2020**, *142*, 105893.
(9) Larrain, M.; Van Passel, S.; Thomassen, G.; Van Gorp, B.; Nhu, T. T.; Huysveld, S.; Van Geem, K. M.; De Meester, S.; Billen, P. Techno-economic assessment of mechanical recycling of challenging post-consumer plastic packaging waste. *Resources, Conservation and Recycling* **2021**, *170*, 105607.
(10) Pérez, R. L.; Ayala, C. E.; Opiri, M. M.; Ezzir, A.; Li, G.; Warner, I. M. Recycling Thermoset Epoxy Resin Using Alkyl-Methyl-Imidazolium Ionic Liquids as Green Solvents. *ACS Applied Polymer Materials* **2021**, *3* (11), 5588−5595.
(11) Bliznakov, E. D.; White, C. C.; Shaw, M. T. Mechanical properties of blends of HDPE and recycled urea-formaldehyde resin. *J. Appl. Polym. Sci.* **2000**, *77* (14), 3220−3227.
(12) Hu, Y.; Gong, M.; Xing, X.; Wang, H.; Zeng, Y.; Xu, C. C. Supercritical water gasification of biomass model compounds: A review. *Renewable and Sustainable Energy Reviews* **2020**, *118*, 109529.
(13) Nastasi, B.; Mazzoni, S.; Groppi, D.; Romagnoli, A.; Astiaso Garcia, D. Solar power-to-gas application to an island energy system. *Renewable Energy* **2021**, *164*, 1005−1016.
(14) Kumar, P.; Pal, N.; Sharma, H. Performance analysis and evaluation of 10 kWp solar photovoltaic array for remote islands of Andaman and Nicobar. *Sustainable Energy Technologies and Assessments* **2020**, *42*, 100889.
(15) Rogers, T. Development of innovation systems for small island states: A functional analysis of the Barbados solar water heater industry. *Energy for Sustainable Development* **2016**, *31*, 143−151.
(16) Nurlatifah; Yamauchi, T.; Nakajima, R.; Tsuchiya, M.; Yabuki, A.; Kitahashi, T.; Nagano, Y.; Isobe, N.; Nakata, H. Plastic additives in deep-sea debris collected from the western North Pacific and estimation for their environmental loads. *Science of The Total Environment* **2021**, *768*, 144537.
(17) Hübner, F.; Brückner, A.; Dickhut, T.; Altstädt, V.; Rios de Anda, A.; Ruckdäschel, H. Low temperature fatigue crack propagation in toughened epoxy resins aimed for filament winding of type V composite pressure vessels. *Polym. Test.* **2021**, *102*, 107323.
(18) Torres-Herrador, F.; Eschenbacher, A.; Blondeau, J.; Magin, T. E.; Geem, K. M. V. Study of the degradation of epoxy resins used in spacecraft components by thermogravimetry and fast pyrolysis. *Journal of Analytical and Applied Pyrolysis* **2022**, *161*, 105397.
(19) Liu, S.; Guo, L.; Jin, H.; Li, L.; Li, G.; Yu, L. Hydrogen production by supercritical water gasification of coal: A reaction kinetic model including nitrogen and sulfur elements. *Int. J. Hydrogen Energy* **2020**, *45* (56), 31732−31744.
(20) Liu, S.; Jin, H.; Wei, W.; Guo, L. Gasification of indole in supercritical water: Nitrogen transformation mechanisms and kinetics. *Int. J. Hydrogen Energy* **2016**, *41* (36), 15985−15997.
(21) Liu, S.; Jin, H.; Yang, Y.; Yu, L. Molecular dynamic investigation on nitrogen migration during hydrogen production by indole gasification in supercritical water. *J. Mol. Liq.* **2021**, *324*, 114769.
(22) Chen, J.; Pan, X.; Li, H.; Jin, H.; Fan, J. Molecular dynamics investigation on the gasification of a coal particle in supercritical water. *Int. J. Hydrogen Energy* **2020**, *45* (7), 4254−4267.
(23) Gong, Y.; Guo, Y.; Wang, S.; Song, W.; Xu, D. Supercritical water oxidation of quinazoline: Reaction kinetics and modeling. *Water Res.* **2017**, *110*, 56−65.
(24) Bai, B.; Liu, Y.; Wang, Q.; Zou, J.; Zhang, H.; Jin, H.; Li, X. Experimental investigation on gasification characteristics of plastic wastes in supercritical water. *Renewable Energy* **2019**, *135*, 32−40.
(25) Bai, B.; Liu, Y.; Meng, X.; Liu, C.; Zhang, H.; Zhang, W.; Jin, H. Experimental investigation on gasification characteristics of polycarbonate (PC) microplastics in supercritical water. *Journal of the Energy Institute* **2020**, *93* (2), 624−633.
(26) Bai, B.; Liu, Y.; Zhang, H.; Zhou, F.; Han, X.; Wang, Q.; Jin, H. Experimental investigation on gasification characteristics of polyethylene terephthalate (PET) microplastics in supercritical water. *Fuel* **2020**, *262*, 116630.
(27) Bai, B.; Jin, H.; Fan, C.; Cao, C.; Wei, W.; Cao, W. Experimental investigation on liquefaction of plastic waste to oil in supercritical water. *Waste Management* **2019**, *89*, 247−253.
(28) Bai, B.; Wang, W.; Jin, H. Experimental study on gasification performance of polypropylene (PP) plastics in supercritical water. *Energy* **2020**, *191*, 116527.
(29) Peng, Z.; Rong, S.; Xu, J.; Jin, H.; Zhang, J.; Shang, F.; Guo, L. Reaction pathways and kinetics for hydrogen production by oilfield wastewater gasification in supercritical water. *Fuel* **2022**, *314*, 123135.
(30) Okolie, J. A.; Nanda, S.; Dalai, A. K.; Kozinski, J. A. Optimization and modeling of process parameters during hydrothermal gasification of biomass model compounds to generate hydrogen-rich gas products. *Int. J. Hydrogen Energy* **2020**, *45* (36), 18275−18288.
(31) Lu, Y. J.; Jin, H.; Guo, L. J.; Zhang, X. M.; Cao, C. Q.; Guo, X. Hydrogen production by biomass gasification in supercritical water with a fluidized bed reactor. *Int. J. Hydrogen Energy* **2008**, *33* (21), 6066−6075.
(32) Wang, C.; Zhu, C.; Cao, W.; Wei, W.; Jin, H. Catalytic mechanism study on the gasification of depolymerizing slag in supercritical water for hydrogen production. *Int. J. Hydrogen Energy* **2021**, *46* (3), 2917−2926.
(33) Ren, C.; Guo, S.; Wang, Y.; Liu, S.; Du, M.; Chen, Y.; Guo, L. Thermodynamic analysis and optimization of auto-thermal supercritical water gasification polygeneration system of pig manure. *Chemical Engineering Journal* **2022**, *427*, 131938.
(34) Chen, J.; Xu, W.; Zhang, F.; Zuo, H.; E, J.; Wei, K.; Liao, G.; Fan, Y. Thermodynamic and environmental analysis of integrated supercritical water gasification of coal for power and hydrogen production. *Energy Conversion and Management* **2019**, *198*, 111927.
(35) Ding, N.; Azargohar, R.; Dalai, A. K.; Kozinski, J. A. Catalytic gasification of glucose to H2 in supercritical water. *Fuel Process. Technol.* **2014**, *127*, 33−40.
(36) Xu, C.; Donald, J. Upgrading peat to gas and liquid fuels in supercritical water with catalysts. *Fuel* **2012**, *102*, 16−25.
(37) Ferreira-Pinto, L.; Silva Parizi, M. P.; Carvalho de Araújo, P. C.; Zanette, A. F.; Cardozo-Filho, L. Experimental basic factors in the production of H2 via supercritical water gasification. *Int. J. Hydrogen Energy* **2019**, *44* (47), 25365−25383.
(38) Cao, C.; Yu, L.; Xie, Y.; Wei, W.; Jin, H. Hydrogen production by supercritical water gasification of lignin over CuO−ZnO catalyst synthesized with different methods. *Int. J. Hydrogen Energy* **2022**, *47* (14), 8716−8728.
(39) Kruse, A.; Meier, D.; Rimbrecht, P.; Schacht, M. Gasification of Pyrocatechol in Supercritical Water in the Presence of Potassium Hydroxide. *Ind. Eng. Chem. Res.* **2000**, *39* (12), 4842−4848.
(40) Zhao, X.; Jin, H.; Chen, Y.; Ge, Z. Numerical study of H2, CH4, CO, O2 and CO2 diffusion in water near the critical point with molecular dynamics simulation. *Computers & Mathematics with Applications* **2021**, *81*, 759−771.
(41) Rodriguez Correa, C.; Kruse, A. Supercritical water gasification of biomass for hydrogen production − Review. *Journal of Supercritical Fluids* **2018**, *133*, 573−590.
(42) Kruse, A.; Dahmen, N. Water − A magic solvent for biomass conversion. *Journal of Supercritical Fluids* **2015**, *96*, 36−45.

https://doi.org/10.1021/acssuschemeng.2c04115
ACS Sustainable Chem. Eng. XXXX, XXX, XXX−XXX